

Mechanical structures for smart-phone enabled sensing

S. Lawes

Faculty of Engineering, the University of Nottingham,
Nottingham, UK
Simon.lawes@nottingham.ac.uk

P Kinnell

School of Mechanical and Manufacturing Engineering,,
Loughborough University, Loughborough, UK
p.kinnell@lboro.ac.uk

Abstract—The paper presents a new strategy for sensor design that is made possible by the usage of ubiquitous mobile devices for signal capture, digitization, and data processing. The approach taken is to design simple mechanical sensor elements such that they produce a sensor output that is easily acquired by a mobile smart device such as a phone or tablet computer. To illustrate this concept, two mechanical displacement transducers have been designed and tested. These sensors make use of displacement amplification structures, Moiré pattern gratings and a double-ended-tuning-fork (DETF) resonant structure. The sensors produced either an acoustic or optical signal in response to an input load or displacement, which can then be acquired using the camera or microphone of a mobile device. The computing power and connectivity of mobile devices makes a wide range of processing, visualisation and storage techniques possible at low cost. Using this technique an optical displacement transducer with a range of 150 μm , and a resolution of $<5 \mu\text{m}$; and an acoustic displacement transducer with a range of 20 μm and a standard error of 0.14 μm , are demonstrated

Keywords—component; passive sensors, Moire fringe, smart phones, compliant mechanisms, acoustic measurement

I. INTRODUCTION

Historically measurement technologies were typically passive, requiring no electrical power or signal conditioning. Elegant mechanisms coupled the measurand to a visual indicator such as a geared dial. However modern transducers have evolved to leverage the sophistication of electronic and computing systems, and now typically require the measurand to be transduced into an electrical signal. This facilitates signal conditioning, other data processing activities such as compensation for environmental factors, and then data transmission. As such, modern sensors require a source of electrical power and signal transmission, which increases the complexity and cost of the sensor significantly. In addition for applications where sensors must remain embedded for long periods in remote or difficult to access places, the additional problems related to long term power of the sensor system may become a significant constraint on potential applications. To address this issue, passive sensors have been a topic of significant research [1,2,3].

A truly passive sensor is able to function by collecting the energy it requires from its local environment. Good examples of simple passive sensors might be a simple mercury thermometer or a colour sensitive litmus paper. Both these devices function in a similar way, for example in the case of the litmus paper, chemical energy is used to trigger a colour

change in the paper, which is then made visible as a result of the ambient light illuminating the paper. Of course the inherent problem with both systems is that the final stage of making a measurement relies on human interpretation to compare the observed output signal against a reference scale. In the examples used these would be either length, or colour respectively. A simple way to remove this level of subjectivity would be to record and digitize the image of the output signal observed by the viewer, then use digital processing techniques to make the comparison in a robust and well defined way [4].

Using these simple and intuitive sensors concepts as an inspiration, this work presents a simple strategy for the development of passive sensors that are specifically designed for integration with a standard mobile device such as a tablet or smart phone. Rather than developing a transducer plus data processing and data transmission capabilities which results in a significant overhead in terms of power, complexity and cost; instead this will be removed from the transducer to an extrinsic mobile device. To make this possible requires the sensing element to successfully transduce the measurand into a signal that is easily acquired by the external device. To achieve this special care must be taken to ensure the transducer is able to provide a viable signal to the mobile device, however, once the data has been acquired by the device it is possible to exploit the significant capability of mobile devices, such as data storage, processing, visualization, and wireless transmission.

To fully illustrate the viability of this concept, and the ability to apply it to extremely challenging measurement applications; two transducers that are able to measure with high precision displacements on the micron and submicron scale have been designed, fabricated, and characterized. These devices are designed to generate output signals that may be acquired by the camera or microphone of a mobile device. In addition techniques for encoding sensor specific information collocated with the transducer such as calibration coefficients, have been developed so they are suitable for retrieval using the camera capability of the mobile device.

To further demonstrate the viability of the approach all the mechanical transducer components created in this work have been designed such that they may easily be directly integrated into metal assemblies such as machines, or structural elements. No special manufacturing processes have been used in the creation of the mechanical components, which have been created using a commercially available laser cutting machine, using 2 mm thick sheets of Stainless Steel 316 or Ti-6AL-4V. The transducers are purely mechanical, highly rugged and

simple to manufacture/assemble. The designs are based on the principles of mechanical displacement amplification [5,6], Moiré fringe patterns of misaligned gratings [7] and acoustic measurement of displacement and strain [8-10].

II. MOIRE FRINGE DISPLACEMENT SENSOR

Measurement and recording of micron scale displacements is traditionally performed by high cost precision instruments such as digital micrometers, linear variable displacement transducers, eddy current or capacitance probes. Interfacing with these sensors requires amplification, analogue to digital conversion and a computer to log or transmit data. We present an opto-mechanical device that can amplify displacements in the range 5-150 μm so that they can be readily observed by eye or by a low cost smart phone camera. The system amplifies displacement through a series of levers with elastic frictionless pivots. The amplified displacement can be used to move a grating relative to another grating which is misaligned. The intersection of the misaligned gratings produces a pattern of interference known as Moiré fringes. In the case of relative translation of the position gratings the Moiré fringes are observed to translate, shifting left to right. With a change in alignment of the gratings the fringe spacing/frequency alters. This can be seen in the nearly aligned and heavily misaligned examples in figure 2.

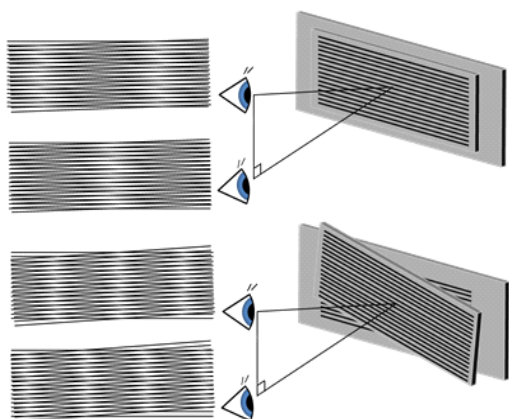


Figure 1 – Examples of Moiré fringes produced by overlapping gratings. The top line of images show a nearly aligned set of gratings viewed from two angles. The bottom line shows a heavily misaligned set of gratings. Note the change of fringe spacing, and insensitivity to viewing angle.

This study is concerned with capturing the measurand with a hand held device. As such it was important that the system be tolerant to changes in the camera position and angle. While fringe position is sensitive to viewing angle the spacing/frequency of fringes is not. Therefore this principle was adopted in this sensor system. Figure 2 shows an early prototype of such a device. The area marked in dashed red indicates the window where fringe patterns can be observed.

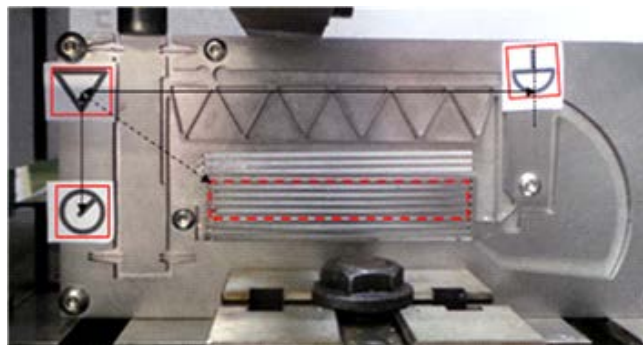


Figure 2 – Image of an early displacement device showing location markers and the window in which Moiré fringe pattern can be observed.

In order to readily process a captured image, and measure fringe spacing, it is necessary to automatically locate this area within an image. Image recognition of primitive patterns allows for a flexible way to locate unique points within an image. The relative position and orientation of these patterns can be used to adjust for image rotation, scale and a degree of skew. Once the fringe window can be easily and repeatedly defined simple numerical methods can be applied to estimate the location of the bright and dark fringes. The principle mechanism was based on finding the brightness of each column of pixels as a series. Two methods were investigated to determine column brightness, average pixel value in a column, and count of pixels above a threshold in each column. The performance of these algorithms depends greatly on prevailing lighting conditions. Flash illumination offers some consistency as well as high contrast and good distinction of grating location, but highly reflective surfaces present uneven distribution of illumination. It was found that sampling a section of the image directly above the pattern window was an effective way to determine a background brightness distribution, which could then be subtracted from the area of interest. Once column values are known, the fringe periodicity could then be determined by FFT to find fundamental frequency or comparing the position of peaks. Figure 3 shows an example device being calibrated. Images were captured with a Samsung Galaxy Camera using flash illumination, at a distance of 45cm, facing normal to the mechanism.

The Samsung Galaxy Camera represents an entry level camera that has smart phone capabilities, such as 3G mobile internet access and access to email, internet connection and the Android App store. A range of displacements from 5-150, in steps of 5, were applied to the input by a Physik Instrumente Precision DC Microdrive. Peak positions were recorded and processed by pixel thresholding after adjustment for background brightness.

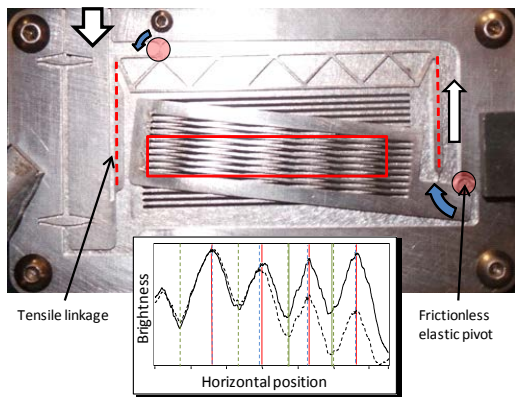


Figure 3 – Illustration of displacement device function, indicating position of joints, tensile linkages and the resulting brightness map. Inset graph shows two plots, the dashed line shows raw brightness values and the solid line data that has been adjusted for background brightness distribution.

The results of this study are shown in figure 4.

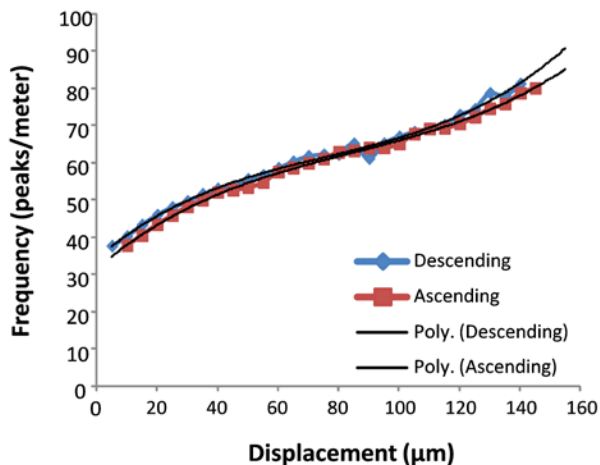


Figure 4 - Graph of the captured spatial frequency of fringes, with units of peaks/metre, plotted against the applied displacement.

Images were collected throughout the experiment and considered fringe spacing for both the loading and unloading case, i.e. for both positive displacement and return to zero, so that that hysteresis could be observed. As can be seen there is minimal disagreement between ascending and descending slopes. These initial studies do not attempt to measure the devices repeatability. It can be seen that these initial measurements suggest a measurement certainty of $\sim 5\mu\text{m}$ over the range of $5\text{-}150\mu\text{m}$, however the approach is just as applicable to much larger or smaller ranges. The lower limit of range is affected by the requirement to measure fringe to fringe spacing to determine period. A minimum grating misalignment is therefore required that presents two fringes within the pattern window. The maximum displacement is limited by the size of the gratings, as a reasonable area of overlap between the gratings must be maintained for all measurement conditions. As such the scale of the gratings misalignment defines a complex relationship between the input displacement and the

scale of the observable output. This flexibility allows for Moiré fringe transducers that can be tailored to the required range, sensitivity, and available size of an application. It is clear that simple design choices can scale a micrometer displacement to an observable window several centimetres in size, making it amenable to capture by low cost camera sensor.

III. DETF ACOUSTIC SENSOR

For the measurement of small displacements with sub-micron uncertainty a double-ended-tuning-fork (DETF) strain sensor was designed. As with the other displacement sensors presented in this work the DETF may also be used to function as a load cell, however in this work the device is characterised by considering an applied displacement only. An image of the sensor is shown in fig 5, mounted to in a test rig. As load applied to the top of the DETF at the load position there is a corresponding modification of the structures' natural frequency. This is a result of the strain developed in within the tines of the DETF structure, such that compressive loads will tend to reduce frequency while tensile loads will increase frequency.

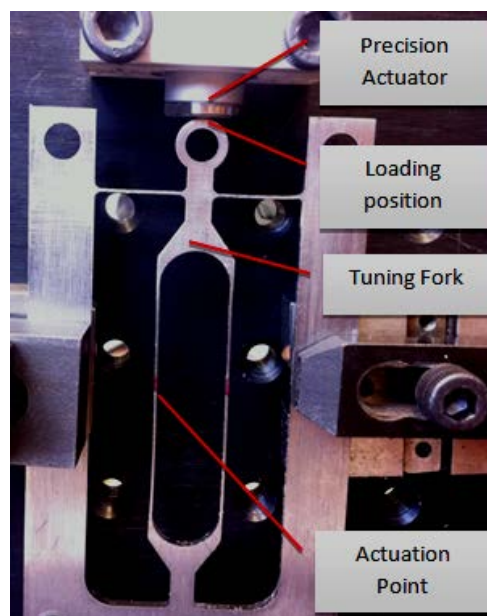


Figure 5 - The DETF resonator mounted within test rig.

The test rig shown in figure 6 used the same Physik Instrumente Microdrive actuator to apply compressive loads to the DETF in the range of $0\text{ to }50\mu\text{m}$. To be able to monitor the frequency of the DETF some excitation must be applied to the tines. This was achieved by plucking one of the tines using a guitar pick at the centre of the tine in a right to left direction. The resulting sound was then sampled using a mobile phone from a distance of approximately 30 cm . In this case the phone used was an Apple iPhone 3, recording standard audio wav files. Using the micro actuator the applied displacement was increased in 2 micrometer steps, with a sound sample taken at each point. The resultant sound signal generated by plucking the DETF is a complex mix of multiple modal frequencies and harmonics. These were sampled using the iPhone and then post processing was applied to clean the audio signal. While this

could be implemented on the iPhone itself, in this work it was done by sending the audio file to a computer where LabVIEW software was used to apply a simple notch filter to the signal designed to accept only frequencies between 800 Hz and 1300 Hz. The LabVIEW tone function was then used to extract the most dominant single tone from this filtered signal. The resulting frequencies are shown in figure 6, the knee in the curve at position A represents the point at which the actuator first makes contact with the DETF. From point A towards point B it can be seen that the frequency decreases as a function of applied displacement until at position B there is a turning point which corresponds with the buckling point of the beams.

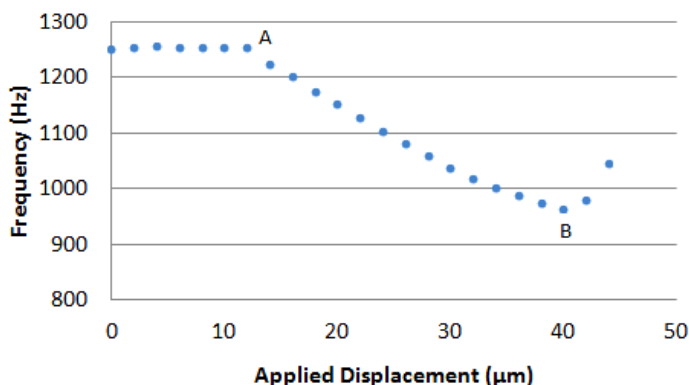


Figure 6 – Graph of the extracted dominant tone plotted against applied displacement.

By fitting a second order curve to the data a relationship linking measured frequency to displacement can be established. As the response curve is clearly non-linear, a second order polynomial was used for this regression analysis, and data from point A (as on figure 6) over a 20 µm range was considered. Over the range a second order regression seems to model the curve well, as can be seen the distribution of the residual errors for this analysis as shown in figure 7.

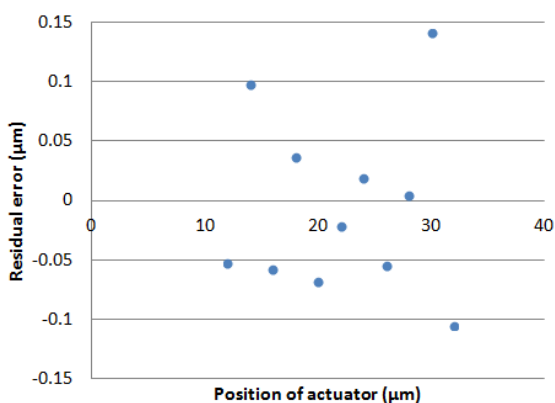


Figure 7 – Graph of residual measurement errors plotted against actuator position.

This was shown to yield a maximum non-linearity of 0.15 % for full scale, which equates to a displacement of 30 nm. To establish the repeatability of the sensor, six repeat readings taken with no load applied, then the sensor was loaded to just beyond buckling (as indicated by point B in figure 7) and a

further 4 readings were taken. Based on these a standard uncertainty of 0.7% of full scale was recorded, which equates to a value of 140 nm.

IV. INTEGRATING DATA THROUGH MACHINE READABLE ID

With a sensor system that makes use of passive transducers and an extrinsic capture system it is important that the individual device can be readily identified and traced. As each transducer may have a different transduction mechanism and will have a unique calibration, the transducer itself is only of use if it can be easily linked to its intrinsic parameters. Traditional labeling could be used to identify samples and relay key parameters but this relies on a human operator to correctly enter sensor information, and any labeling would be at risk of damage over time. Quick recognition (QR) codes offer a simple way to convey relatively short, typically 15-256 ASCII characters. Encoding and decoding exists within an open standard, and includes bit redundancy and scalable error checking. In keeping with the rugged design of these laser cut transducers a design of QR code is proposed which can be readily produced in laser cut sheet metal. Figure 8 shows two possible approaches.

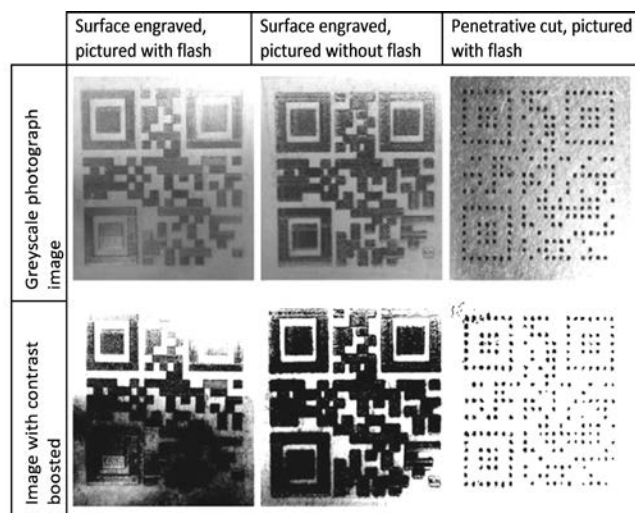


Figure 8 – Image capture and processing for various conditions showing suitability for QR code decoding

QR code reading relies upon contrast between bits in a 2 dimensional barcode. Producing good contrast for these features in metal components can be performed by surface engraving, or by penetrative cuts. A clear bit contrast is required for QR code identification and decoding. Surface engraved bits can be readily achieved but suffer from the high reflectivity where the engraved bits have been surface remelted. That reflectivity can cause some bits to be incorrectly identified. By contrast the penetrative cuts provide contrast from deep nonreflecting features, but are more difficult to produce. Where 'white' bits are surrounded by 'black' it is necessary to provide some mechanical support. As such a grid of supporting material must be maintained. Standard QR code algorithms will not perceive the resulting array of isolated points as a valid QR code. To overcome this challenge a simple

morphological filter can be applied to the captured image, pixel dilation. Dilation is a pixel by pixel operation that expands regions of one value into their neighbouring pixels. Figure 9 shows an example of how dilation operates. This process can be used to grow the small black features until they match the required bit size. Various methods exist for determining which neighbour pixels are affected. The method chosen for this procedure encourages final features which are square in shape to better match the original QR code.

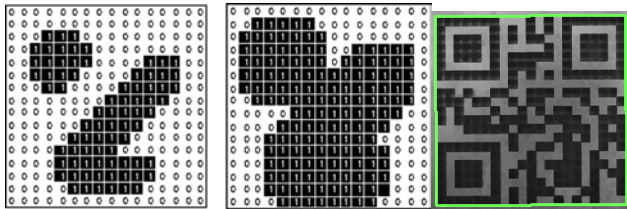


Figure 9 – Images left and centre illustrate the dilation process. The image on the right shows an image of a QR code pattern that has been produced by penetrative cuts and then dilated to produce a readable QR code.

The final processed image is then amenable to industry standard QR decoding. By including a unique camera readable ID with each transducer the collection of sensor data can be easily linked to a sensor profile and data log. The nature of smart devices, as highly connected wireless systems, makes it very straightforward to store and manage data centrally or in a service cloud.

V. CONCLUSIONS

This work has presented a novel concept for the development of a class of sensors that are specifically designed such that as far as possible, power sources, signal amplification, data processing, data storage, and data transmission, may be extrinsic to the sensing element. The specific novelty lies in the design of elegant mechanical structures that are able to convert subtle hard to detect input signals into robust easily captured output signals compatible with mobile devices.

To demonstrate the technical feasibility of this approach, two examples of high resolution displacement sensors have been presented. These were designed to transduce input displacement signals to provide an output signal that may be easily and remotely detected by a standard mobile device such as a smart phone. Using this approach an optical displacement transducer with a range of 150 μm , and a resolution of $<5 \mu\text{m}$, and an acoustic displacement transducer with a range of 20 μm , a nonlinearity (from a second order polynomial fit) of 30 nm, and a standard error of 0.14 μm , are demonstrated.

The results demonstrated in this work were collected under laboratory conditions, as such more in depth real-life testing is required to understand the limitations of the approach. However, while the devices presented in this work are early stage prototypes, they clearly demonstrate the ability to create

simple, mechanically robust, low cost devices that through integration with a mobile device are able to generate high performance measurements.

We envisage further development of this approach, with a wide range of possible applications. For example it may be possible to integrate similar devices within structural elements such as machine chassis, building materials [11], or tooling and fixtures for manufacturing [12], or external fixation devices using in medical applications [13]. Once in place these devices would enable maintenance engineers, building surveyors, or medical practitioner to interrogate the sensors with their own standard smart phone or tablet. With this in mind next steps for this work are to establish how robust the approach is likely to be if deployed with variable smart phones, which are operated by multiple users.

REFERENCES

- [1] L. Ruiz-Garcia, L. Lunadei, P. Barreiro, I. Robla 2009. "A Review of Wireless Sensor Technologies and Applications in Agriculture and Food Industry: State of the Art and Current Trends." *Sensors* 9, no. 6: 4728-4750
- [2] F. Khoshnoud, C. W. de Silva, "Recent advances in MEMS sensor technology – biomedical applications," *Instrumentation & Measurement Magazine, IEEE*, vol.15, no.1, pp.8,14, February 2012
- [3] A. J. Knobloch, R. Faisal, D. Ahmad, W. Sexton, and D. W. Vernooy. "Remote Driven and Read MEMS Sensors for Harsh Environments." *Sensors* 13, no. 10 (2013): 14175-14188.
- [4] A. K. Yetisen, J. L. Martinez-Hurtado, A. Garcia-Melendrez, F. da Cruz Vasconcellos, C. R. Lowe, A smartphone algorithm with inter-phone repeatability for the analysis of colorimetric tests, *Sensors and Actuators B: Chemical*, Volume 196, June 2014, Pages 156-160
- [5] S. B. Choi, S. S. Han, Y. M. Han, and B. S. Thompson. "A magnification device for precision mechanisms featuring piezoactuators and flexure hinges: Design and experimental validation." *Mechanism and Machine Theory* 42, no. 9 (2007): 1184-1198..
- [6] S. Kota, Compliant systems using monolithic mechanisms. *Smart Materials Bulletin*. 2001(3): p. 7-10.
- [7] J. T. M. Stevenson, J.R. Jordan, Metrological gratings and Moire fringe detection methods for displacement transducer. *Physical Science, Measurement and Instrumentation, Management and Education, IEE Proceedings A*, 1989, 136 (5).
- [8] T. Ueda, F. Kohsaka, and E. Ogita. "Precision force transducers using mechanical resonators." *Measurement* 3, no. 2 (1985): 89-94.
- [9] T. Yan, B. E. Jones, R. T. Rakowski, M. J. Tudor, S. P. Beeby, and N. M. White. "Design and fabrication of thick-film PZT-metallic triple beam resonators." *Sensors and Actuators A: Physical* 115, no. 2 (2004): 401-407..
- [10] T. Hayashi, K. Yoshihisa, U. Kazunaga, H. Tsuyoshi, S. Hiroshi, and K. Masaaki. "Evaluation of tuning fork type force transducer for use as a transfer standard." *Measurement* 41, no. 9 (2008): 941-949.
- [11] J. M. Ko, Y. Q. Ni. "Technology developments in structural health monitoring of large-scale bridges." *Engineering structures* 27, no. 12 (2005): 1715-1725.
- [12] D. Ceglarek, J. Shi. "Fixture failure diagnosis for autobody assembly using pattern recognition." *Journal of Engineering for Industry* 118, no. 1 (1996): 55-66.
- [13] J. B. Richardson, J. L. Cunningham, A. E. Goodship, B. T. O'connor, and J. Kenwright. "Measuring stiffness can define healing of tibial fractures." *Journal of Bone & Joint Surgery, British Volume* 76, no. 3 (1994): 389-394.